

## ***How Can Present and Future Satellite Missions Support Scientific Studies that Address Ocean Acidification?***

The Faculty of Oregon State University has made this article openly available.  
Please share how this access benefits you. Your story matters.

<b>Citation</b>	Salisbury, J., Vandemark, D., Jönsson, B., Balch, W., Chakraborty, S., Lohrenz, S., ... & Yates, K. (2015). How Can Present and Future Satellite Missions Support Scientific Studies that Address Ocean Acidification?. <i>Oceanography</i> , 28(2), 108-121. doi:10.5670/oceanog.2015.35
<b>DOI</b>	10.5670/oceanog.2015.35
<b>Publisher</b>	Oceanography Society
<b>Version</b>	Version of Record
<b>Terms of Use</b>	<a href="http://cdss.library.oregonstate.edu/sa-termsfuse">http://cdss.library.oregonstate.edu/sa-termsfuse</a>

# How Can Present and Future Satellite Missions Support Scientific Studies that Address Ocean Acidification?

By Joseph Salisbury, Douglas Vandemark, Bror Jönsson, William Balch, Sumit Chakraborty, Steven Lohrenz, Bertrand Chapron, Burke Hales, Antonio Mannino, Jeremy T. Mathis, Nicolas Reul, Sergio R. Signorini, Rik Wanninkhof, and Kimberly K. Yates



**FIGURE 1.** Some satellites used to study the ocean carbonate system. The orientations and orbits of the spacecrafts are not to scale.

**ABSTRACT.** Space-based observations offer unique capabilities for studying spatial and temporal dynamics of the upper ocean inorganic carbon cycle and, in turn, supporting research tied to ocean acidification (OA). Satellite sensors measuring sea surface temperature, color, salinity, wind, waves, currents, and sea level enable a fuller understanding of a range of physical, chemical, and biological phenomena that drive regional OA dynamics as well as the potentially varied impacts of carbon cycle change on a broad range of ecosystems. Here, we update and expand on previous work that addresses the benefits of space-based assets for OA and carbonate system studies. Carbonate chemistry and the key processes controlling surface ocean OA variability are reviewed. Synthesis of present satellite data streams and their utility in this arena are discussed, as are opportunities on the horizon for using new satellite sensors with increased spectral, temporal, and/or spatial resolution. We outline applications that include the ability to track the biochemically dynamic nature of water masses, to map coral reefs at higher resolution, to discern functional phytoplankton groups and their relationships to acid perturbations, and to track processes that contribute to acid variation near the land-ocean interface.

## INTRODUCTION

Ocean acidification (OA) is defined as a persistent change to inorganic ocean carbon chemistry caused by the flux of atmospheric anthropogenic CO<sub>2</sub> into the upper ocean. The overriding concern for the ocean is the probability that OA and compounding regional processes that modify acid variability may have detrimental effects on fisheries, coral reefs, and ultimately coastal ecosystems and economies.

The rate of CO<sub>2</sub> increase in the ocean has been reasonably well quantified at the global scale (e.g., Sabine and Tanhua, 2010; Feely et al., 2012). Surface water partial pressure of CO<sub>2</sub> ( $p\text{CO}_2$ ) is increasing by  $\sim 2 \mu\text{atm yr}^{-1}$ , at nearly the same rate as atmospheric  $p\text{CO}_2$  (Le Quéré et al., 2014). Because seawater is alkaline and therefore buffered, increasing CO<sub>2</sub> causes a relatively modest decrease in pH. Nevertheless, upper-ocean pH is still decreasing by  $\sim 0.002 \text{ yr}^{-1}$  (seawater is well buffered for CO<sub>2</sub>, so the rising CO<sub>2</sub> does not rapidly lower the pH; see references above). A coupled carbonate system variable, the aragonite saturation state ( $\Omega_{\text{arag}}$ ), is also decreasing by  $\sim 0.01 \text{ yr}^{-1}$ . Aragonite is a calcite mineral directly related to seawater carbonate ion concentration. It is widely believed that if  $\Omega_{\text{arag}}$  decreases to values near 1.0, many ocean organisms will be stressed as this shell-building substance becomes unstable and nears

dissolution. The rate of change in each of these OA indicators will accelerate with any increase in atmospheric CO<sub>2</sub> loading and with an expected decrease in ocean buffering capacity. A primary regional concern is in high-latitude oceans where cold water and lower buffering translate to more rapid change. Assuming business-as-usual CO<sub>2</sub> emission scenarios, predictions indicate perennial aragonite undersaturation at polar and subpolar latitudes by the end of the twenty-first century (IPCC, 2013).

Arguably, the greatest impacts of OA are likely to occur in coastal regions (e.g., Cooley et al., 2009; Mathis et al., 2014). Near the coasts, numerous additional processes lead to increased complexity in carbonate dynamics (Cai et al., 2010; Cross et al., 2013). These factors include acidic inputs from rivers (Salisbury et al., 2008), upwelling (Feely et al., 2008), intense biological respiration fueled by productivity (Cai et al., 2010), and atmospheric deposition from continental sources (Doney et al., 2009). Many coastal ecosystems experience large magnitude changes in the carbonate system over short time scales (Waldbusser and Salisbury, 2014). These changes, when combined with longer-term OA or other stressors (e.g., temperature), can have deleterious compounding effects on organisms and ecosystems (Breitburg et al., 2015, in this issue). There is still large

uncertainty in our ability to predict these effects, and it has also become apparent that upper-ocean inorganic carbon cycle dynamics are substantial in both space and time. Observation and modeling at many spatial and temporal scales are needed to better understand the ranges of natural (i.e., pre-industrial) and human-impacted carbon system variations and how they relate to OA and its potential impacts.

Ocean observations of the inorganic carbonate system have been central in defining current understanding about OA and underlying seawater chemistry. When combined with appropriate calibration and validation data sets, traditional in situ measurements and autonomous sensors on ships, moorings, and profiling floats can help to monitor global-scale and seasonal trends in carbonate system variables and, over the longer term, OA (Takahashi et al., 2014). One key tool supporting future prediction as well as resolving the range of carbonate system variability is ocean remote sensing, particularly when applied to determining biochemical and physical processes that relate to OA (Figure 1).

Satellite data provide synoptic, calibrated, and cost-effective measurements for investigating processes across spatio-temporal scales that are infeasible with ground-based approaches. Satellite sensors measuring surface temperature, color, wind, salinity, and sea surface height have enabled a fuller understanding of physical, chemical, and biological phenomena driving OA and its impacts on ecosystems. These data allow environmental monitoring at spatial scales of  $\sim 10 \text{ m}$  to  $\sim 1,000 \text{ km}$ , and temporal scales from hours to decades. Recent missions designed to retrieve salinity and a variety of other variables are poised to revolutionize our understanding of the physical and biogeochemical processes that modulate OA. Satellite methods are being devised to allow spatial interpolation of relatively sparse surface carbon measurements (e.g., alkalinity and  $p\text{CO}_2$ ) by exploiting correlations with temperature, salinity, and other factors



(Hales et al., 2012; Signorini et al., 2013; Velo et al., 2013). In addition, numerous processes tied to carbonate system variation can be resolved via measurement from different bands in the electromagnetic spectrum as acquired using the current suite of space-based sensors (examples in Figures 1 and 2 and Table 1). For example, riverine and groundwater tracers can be measured in the coastal ocean using new satellite-based salinity sensors (e.g., Salisbury et al., 2011; Gierach, et al., 2013). Ocean color data can be used to detect distinct signatures associated with freshwater inputs to many coastal locations (e.g., Del Castillo et al., 2008). Upwelling signals are readily identified through sea surface temperature (SST) anomalies (e.g., Hormazabal et al., 2001), wind stress curl, or via field-based algorithms relating temperature and ocean color (e.g., Lefèvre et al., 2002). Satellite sensors measuring surface temperature, wind, salinity, and height have enabled a fuller understanding of phenomena that control biochemical variability. By virtue of their covariance with ocean color, many biological processes affecting OA can be diagnosed with satellite data.

Here, we update and expand on

previous work that shows the benefits of space-based assets for OA studies. Direct OA monitoring at the decadal scale via satellite-based  $p\text{CO}_2$  approaches may become feasible in the future, but the main focus here is on use of satellite data to better determine the processes controlling OA and surface ocean carbonate system variability. Synthesis of present satellite data streams is described, as are opportunities that will become available using satellite sensors with increased spectral, temporal, or spatial resolution. These sensors will provide new capabilities to track the dynamic nature of water masses, map coral reefs at higher resolution, map functional phytoplankton groups and their relationship to OA, and better understand processes contributing to carbonate system variability occurring at the land-ocean interface.

### TRACKING THE CARBONATE SYSTEM

Satellites do not directly measure chemistry; rather, satellite observables can be used as purely statistical proxies of carbonate, or as elements in quasi-mechanistic chemical reconstructions when combined with in-water

observations. We review the utility of satellite observations in this endeavor.

The carbonate system is controlled by two combined variables, total dissolved carbonic acid ( $T_{\text{CO}_2}$ ) and titration alkalinity ( $T_{\text{alk}}$ ).  $T_{\text{CO}_2}$  has a concentration of  $\sim 2,000 \mu\text{mol kg}^{-1}$ , distributed across the species  $\text{CO}_2^*$  (the sum of concentrations of aqueous  $\text{CO}_2$  and carbonic acid), bicarbonate [ $\text{HCO}_3^-$ ], and carbonate [ $\text{CO}_3^{2-}$ ], with relative contributions listed below each individual species:

$$T_{\text{CO}_2} = \underset{\sim 1\%}{\text{CO}_2^*} + \underset{\sim 90\%}{[\text{HCO}_3^-]} + \underset{\sim 9\%}{[\text{CO}_3^{2-}]}$$

For nominal surface waters with  $T = 18^\circ\text{C}$  and  $S = 35$ ,  $T_{\text{alk}}$  has a concentration of  $\sim 2,300 \mu\text{mol kg}^{-1}$ , distributed as follows:

$$T_{\text{alk}} = \underset{\sim 80\%}{[\text{HCO}_3^-]} + \underset{\sim 16\%}{2[\text{CO}_3^{2-}]} + \underset{\sim 4\%}{[\text{B}(\text{OH})_4^-]} + \underset{\sim 0.2}{[\text{OH}^-]} - \underset{\sim 0.0004\% \dots}{[\text{H}^+]}$$

+ minor bases – minor acids.

Absolute values of neither  $T_{\text{CO}_2}$  nor  $T_{\text{alk}}$  are considered drivers of ecosystem OA responses, while chemical subspecies are more biologically important, particularly  $\text{CO}_2^*$ ,  $[\text{H}^+]$  (via pH), and  $\text{CO}_3^{2-}$  (via  $\Omega$ ;  $\Omega = [\text{CO}_3^{2-}][\text{Ca}^{2+}]/K'_{\text{sp,m}}$ , where  $[\text{Ca}^{2+}]$  is the concentration of dissolved calcium in

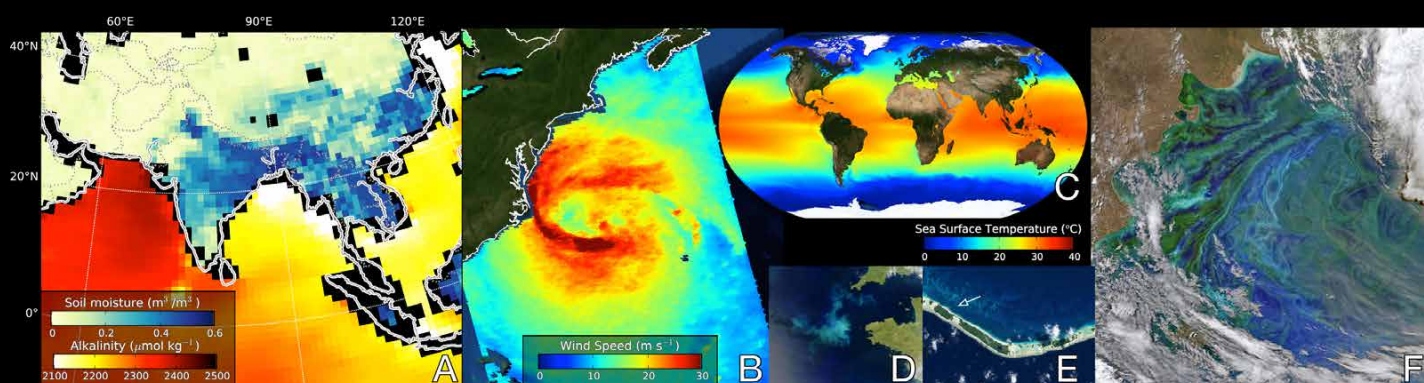


**FIGURE 2.** Satellite data relevant to the carbonate system. (A) Soil moisture from the Aquarius Mission shown together with alkalinity based on Aquarius sea surface salinity (SSS), MODIS/Aqua sea surface temperature (SST), and a surface  $T_{\text{alk}}$  algorithm by Lee et al. (2006). The patterns of high soil moisture and low  $T_{\text{alk}}$  illustrate how land processes can affect coastal  $T_{\text{alk}}$  and help to understand end-member mixing. (B) Surface winds from OSCAT/OceanSat-2 October 29, 2012, showing Hurricane Sandy. Radar scatterometry enables subdaily wind observations, helping to better determine air-sea flux of  $\text{CO}_2$ . (C) Global SST from MODIS/Aqua. Such data are critical for estimating solubility of  $\text{CO}_2$  and calcite in the surface ocean. (D) Coccolith bloom off Brittany, France, June 15, 2004, MODIS/Aqua. This formation of particulate inorganic carbon represents an alkalinity sink that is observable from space. *Jacques Desclouitres, NASA/GSFC* (E) Landsat-7 visible image of the Rangiroa Atoll, French Polynesia, after extreme bleaching in 1998. High-resolution imagery allows mapping of coral distributions and health (Mumby et al., 2001). *Serge Andréfouët, NASA/VisibleEarth* (F) VIIRS false color image off the Patagonian Shelf with color signatures from dinoflagellates, diatoms, and coccolithophores. These functional phytoplankton groups have differing effects on surface  $T_{\text{CO}_2}$  and  $T_{\text{alk}}$ . Bands of color can reveal eddies and currents. *Norman Kuring NASA/GSFC*

**TABLE 1.** A sampling of current satellite missions relevant to measuring ocean acidification (OA)-related parameters and processes affecting OA. The table is not intended to be inclusive.

Satellite	Agency Name	Sensor	Wavelengths	Geophysical Measurement	Effective Repeat Interval	Product Spatial Resolution (km)	Orbit	Launch Date	Notes
<b>OCEAN COLOR   APPLICATION:</b> Chlorophyll, particulate and dissolved colored carbon, particulate inorganic carbon, primary and net community productivity, $p\text{CO}_2$									
Aqua and Terra	NASA	Moderate Resolution Imaging Spectroradiometer (MODIS)	Visible – near infrared	Water leaving radiance ( $\lambda$ )	~ daily	0.25, 0.50, and 1.00	Polar	1999 (Terra) 2002 (Aqua)	
Suomi-NPP	US National polar orbiting partnership	Visible Infrared Radiometer Suite (VIIRS)	Visible – near infrared	Water leaving radiance ( $\lambda$ )	~ daily	0.75	Polar	2011	
MERIS	European Space Agency	MEdium Resolution Imaging Spectrometer (MERIS)	Visible – near infrared	Water leaving radiance ( $\lambda$ )	~ daily	0.3	Polar	2002	
COMS	Korea Ocean Satellite Center	Geostationary Ocean Colour Imager (GOCI)	Visible – near infrared	Water leaving radiance ( $\lambda$ )	1 hour	0.5 (at nadir)	Geostationary	2009	
OceanSat 2	Indian Space Research Organisation	Ocean Colour Monitor (OCM)	Visible – near infrared	Water leaving radiance ( $\lambda$ )	~ daily	0.36	Polar	2009	
<b>SEA SURFACE TEMPERATURE   APPLICATION:</b> Temperature, solubility of carbon dioxide, solubility of calcite minerals, $p\text{CO}_2$									
Several since 1978	NOAA	Advanced Very High Resolution Radiometer (AVHRR)	Infrared (~12 $\mu\text{m}$ )	IR radiance	Each ~ daily	1.1	Polar	Several; 1978–present	Four presently commissioned
Geostationary Operational Environmental Satellite (GOES)	NOAA	GOES Imagers	Infrared (~12 $\mu\text{m}$ )	IR radiance	Each hourly	0.75	Geostationary	Several; 1975–present	Three presently commissioned; one in holding orbit
Aqua and Terra	NASA	MODIS	Infrared (3.5 to 4.2 $\mu\text{m}$ )	IR radiance	Each ~ daily	1	Polar	1999 (Terra) 2002 (Aqua)	
Meteosat Second Generation	ESA	Spinning Enhanced Visible and InfraRed Imager (SEVIRI)	Infrared	IR radiance	3-hourly	11.16 (at nadir)	Geostationary	Several; 2008–present	Three presently commissioned
Tropical Rainfall Measuring Mission's (TRMM)	NASA and JAXA	Microwave Imager (TMI)	Microwave (10.7 GHz)	Passive microwave emissivity	3-day average	25	Polar	1997	
Suomi-NPP	US National polar orbiting partnership	VIIRS	Infrared	IR radiance	~ daily	0.75	Polar	2011	
<b>CORAL REEF AND COASTAL MAPPING   APPLICATION:</b> Coral reef area, coral reef health, shallow water resuspension, near coastal processes									
Landsat-type; several since 1972	USGS	Operational Land Imager (OLI) on Landsat 8 is the latest	Visible – near infrared	Earth and water leaving radiance (I)		0.03	Polar	Several since 1972	Two presently commissioned
MERIS	European Space Agency	Medium Resolution Imaging Spectrometer	Visible – near infrared	Water leaving radiance (I)	~ daily	0.3	Polar	2002	0.25 km product may be suitable for mapping
Aqua and Terra	NASA	MODIS	Visible – near infrared	Water leaving radiance (I)	~ daily	0.25, 0.50, and 1.00	Polar	1999 (Terra) 2002 (Aqua)	0.30 km product may be suitable for mapping
Satellite Pour l'Observation de la Terre (SPOT)	CNES (Centre national d'études spatiales)	Spot XS	Visible – near infrared	Earth and water leaving radiance (I)	5–25 days	0.02	Polar	Several since 1986	
Quick Bird 2	Digital Globe (Commercial)	Digital Globe Constellation	1 visible, 1 near infrared	Earth and water leaving radiance (I)	3 days	0.005	Polar	2001	
RapidEye Earth Imaging System (REIS)	RapidEye (Commercial)	RapidEye Constellation	2 visible, 1 near infrared	Earth and water leaving radiance (I)	Several days	~0.010	Polar	2008	

Table continues on next page...

TABLE 1. Continued...

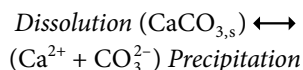
Satellite	Agency Name	Sensor	Wavelengths	Geophysical Measurement	Effective Repeat Interval	Product Spatial Resolution (km)	Orbit	Launch Date	Notes
<b>SOIL MOISTURE/WATER BUDGETS</b>   APPLICATION: Region scale water cycle studies, freshwater flux to the ocean, soil moisture									
Gravity Recovery and Climate Experiment (GRACE)	NASA	Several instruments	N/A	Microwave ranging distance/ accelerometer	~monthly	~300	Polar	2002	Several follow on missions planned
GCOM-W1	Japan Aerospace Exploration Agency (JAXA)	AMSR-2	C-Band microwave (6.9 and 10.6 Ghz)	Passive microwave radiation	2–3 days	~56	Polar	2012	Primarily for soil moisture; limited use for salinity
Soil Moisture Active Passive (SMAP)	NASA	Microwave radiometer/ Synthetic aperture radar	1.4 GHz radiometer/ 1.3 Ghz radar	Microwave emissivity and backscatter	3 day	~3–47	Polar	2015	
<b>ALTIMETRY</b>   APPLICATION: Sea Surface height, ocean currents, river stage height, mixing, $p\text{CO}_2$									
Ocean Surface Topography Mission (OSTM)/ Jason-2	NASA/ CNES/ NOAA	Poseidon-3	Pulsed radar altimeter	Reflectance at 13.6 and 5.3 GHz	~10 day average	~310 track spacing	Geocentric	2008	
<b>SALINITY SENSORS</b>   APPLICATION: Ocean surface Salinity, total alkalinity, $\text{CO}_2$ and calcite mineral solubility, mixing									
Soil Moisture Ocean Salinity (SMOS)	ESA	Microwave Imaging Radiometer with Aperture Synthesis (MIRAS)	L-Band microwave (1.4 Ghz)	Passive microwave radiation	10–30 day average	~75	Polar	2009	Also used for soil moisture
Satélite de Aplicaciones Científicas (SAC)-D,	NASA/ Comisión Nacional de Actividades Espaciales (CONAE)	Aquarius	L-Band microwave (1.3 Ghz)	Passive microwave radiation	10–30 day average	~100	Polar	2011	Also used for soil moisture
<b>SCATTERMETERS/RADIOMETERS</b>   APPLICATION: Wind speed, air sea flux, mixing $p\text{CO}_2$									
USAF F-16 through F-18	US Air Force (DMSP)	Special Sensor Microwave Imager/Sounder (SSM/IS)	Various microwave 19 to 183 GHz	Passive microwave radiation	Sub daily	17–74	Polar	2005	Also used for SST
MetOp-B	European Space Agency	Advanced SCATterometer (ASCAT)	5.255 GHz (C-band)	Active radar	29 days	25–50	Polar	2012	
<b>ATMOSPHERIC CARBON DIOXIDE</b>   APPLICATION: Air-sea $p\text{CO}_2$ disequilibrium									
Orbiting Carbon Observatory-2 (OCO-2)	NASA	Triple spectrometers	NIR	Absorption (I)	16 days	1,000	Polar	2014	Full column $\text{CO}_2$

seawater, and  $K'_{\text{sp,m}}$  is the solubility product of the carbonate mineral).

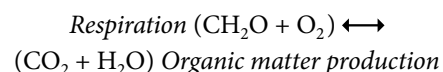
Distributions of chemical subspecies are set by acid-base equilibration, and thermodynamic relations are well known. Distributions can be calculated provided any two of the measurable parameters are both well known (e.g., Zeebe and Wolf-Gladrow, 2001). The first-order effects come from shifts in the ratio of  $T_{\text{CO}_2}:T_{\text{alk}}$ , with lower pH, higher  $\text{CO}_2^*$ , and lower  $\Omega$  conditions driven by higher  $T_{\text{CO}_2}:T_{\text{alk}}$  and basic conditions from the opposite.

### PROCESSES AFFECTING $T_{\text{CO}_2}:T_{\text{alk}}$

Processes affecting  $T_{\text{CO}_2}$  and  $T_{\text{alk}}$  can be characterized as biological (shell and organic matter production and remineralization) or physical (mixing, evaporation, and dilution) and occur at a variety of temporal and spatial scales (Figure 3). The biological reactions can be schematically represented simply:



and



Precipitation incorporates impurities such as  $\text{Mg}^{2+}$  or other cations, and there are multiple forms of solid  $\text{CaCO}_3$ . Organic matter is not as simple as shown above, and a variety of nutrients (N, P, Si, trace elements) play essential roles in organic matter production, while the respiration reaction can take advantage of a number of oxidizing agents in addition to  $\text{O}_2$ .

Nonetheless, these reactions capture features that drive carbonate-system response. Precipitation consumes  $T_{CO_2}$  and  $T_{alk}$ , but affects  $T_{alk}$  twice as much as  $T_{CO_2}$ , and the chemistry of waters in which it occurs exhibits a decreasing  $T_{CO_2}:T_{alk}$  ratio and thus an acidic response with lower pH and  $\Omega$ , and higher  $CO_2^*$ . Organic matter production primarily decreases the abundance of  $T_{CO_2}$ , and the waters in which it occurs show a lower  $T_{CO_2}:T_{alk}$  ratio and thus a basic response with higher pH and  $\Omega$ , and lower  $CO_2^*$ . (The  $T_{alk}$  effect is at most ~15% of the  $T_{CO_2}$  consumption, depending on the form of associated N.) As was the case with the definitions and equilibrium constraints, these effects are well constrained (e.g., Sarmiento and Gruber, 2006).

Mixing causes conservative distributions of T, S,  $T_{CO_2}$ , and  $T_{alk}$ , reflecting fractional contributions of end members. In some extreme cases with very different end members, such as estuaries and river plumes, the combinations of these co-varying factors can lead to large departures of the individual chemical species from conservative behavior; however, in the ocean interior, mixing effects are relatively small and difficult to detect.

Satellite retrieval of particulate organic carbon (POC), chlorophyll (Chl), or particulate inorganic carbon (PIC), yields information on the net result, not just of production/remineralization balances, but also of other removals or concentrations like particle sinking or physical dispersion or convergence. New salinity sensors along with those for SST provide proxies for mixing, but all are limited in that the snapshots do not capture the rates or the initial or end member chemistry conditions that determine actual carbonate system distributions corresponding to the satellite products. In practice, statistical and semi-empirical models, coupled with in-water ground-truth observations, are required to generate OA-relevant satellite-based carbonate-system products.

Detection of perturbations in the carbonate chemistry based on remotely observable parameters is more

challenging. Although geologically extreme, the rising  $T_{CO_2}$  and alteration of carbonate chemistry via rising  $T_{CO_2}:T_{alk}$  ratios, driven by rising atmospheric  $CO_2$ , is small relative to, for example, seasonal variability. Direct effects of rising  $CO_2$  are hypothetical at this point, and include the potential for stimulation of primary producers in low- $CO_2$  waters, or suppression of calcifying species in high- $CO_2$  waters. While mechanistically feasible and logically compelling, the community has not yet demonstrated empirical linkages between anthropogenically elevated  $CO_2$  and remotely observable parameters. The utility of remote-sensing algorithms is presently in the ability to parameterize hydrographic linkages to natural variability and to bolster our understanding of baseline conditions.

### STATE OF THE ART IN REMOTE SENSING OF CARBONATE SYSTEM VARIABILITY

Although remote-sensing tools for studying surface temperature variability and its subsequent thermodynamic effects on the ocean carbonate system have existed for decades, the practice of combining

satellite data streams to study physical and biological variability is a relatively recent development (Gledhill et al., 2009). Several sensors have been launched since 2010, including a new generation of sensors for surface salinity that promise to provide further opportunities for enhancing syntheses and envisioning new applications.

Investigations of carbonate system variability and its effects on OA can be separated into chemical, physical, and biological forcing and the resulting impacts on ecosystems. Remote sensing can be categorized in the same fashion, recognizing that some sensors can be used to study both forcing and impacts. Remotely sensed chemical forcing includes melded multisensor and model estimates of  $pCO_2$  and air-sea  $CO_2$  fluxes (Rödenbeck et al., 2013), and estimates of alkalinity that rely heavily on remotely sensed salinity. Water mass, ocean currents, and ecological province designations (e.g., Hardman-Mountford et al., 2008) can be gleaned from temperature, altimeter, and visible spectrum sensors. Ecological responses can be estimated from satellite products including Chl, PIC, and productivity,

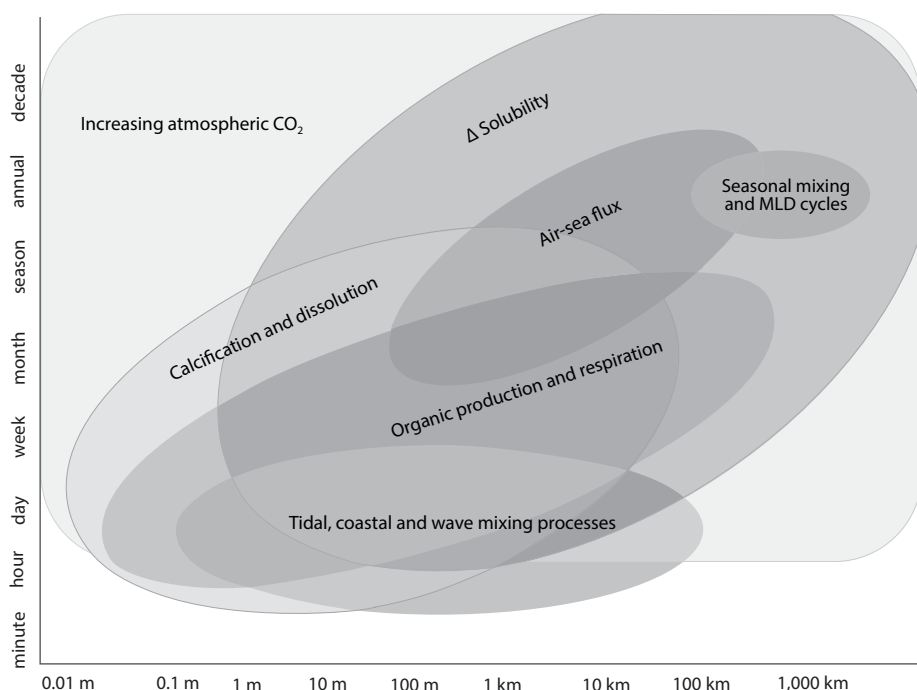


FIGURE 3. Approximate scales of processes affecting important carbonate parameters. MLD = mixed layer depth.



relying heavily on sensors also measuring in the visible spectrum. Details are provided below; see Figures 4 and 5.

## REMOTE SENSING OF TOTAL ALKALINITY

Global monitoring of surface ocean  $T_{\text{alk}}$  is now arguably the most viable application of remote sensing in support of carbonate system and OA studies because  $T_{\text{alk}}$  is only weakly impacted by biological processes, it is strongly covariant with seawater salinity, and there is now continuous access to surface salinity observations from space (Land et al., 2015). Moreover, Lee et al. (2006) and others show that a nonlinear combination of salinity and SST measurements can further resolve remaining nonconservative variation in  $T_{\text{alk}}$  estimates. First-order global  $T_{\text{alk}}$  data should be forthcoming, given monthly SSS data products from the Soil Moisture and Ocean Salinity (SMOS) and Aquarius (Reul et al., 2013; Lagerloef et al., 2013) satellites and widely utilized satellite SST

products.  $T_{\text{alk}}$  product characteristics will enfold the 50–150 km spatial resolution and imprecision in salinity data; for example,  $\pm 0.2$  in satellite-derived salinity translates to  $\pm 10\text{--}15 \mu\text{Mol kg}^{-1}$  in  $T_{\text{alk}}$ . Validation of such first-order surface ocean  $T_{\text{alk}}$  estimates will make use of growing discrete sampling databases such as the Global Data Analysis Project (GLODAP; Key et al., 2004). A likely contribution from satellite-informed total alkalinity products will be the identification of mixing regions and  $T_{\text{alk}}:S$  dynamics near salinity fronts that are now poorly resolved in climatologies and/or in situ global gridded  $T_{\text{alk}}$  products. Refining  $T_{\text{alk}}$  estimates in these regions requires additional information to help resolve non-conservative  $T_{\text{alk}}:S$  variation due to biochemically diverse freshwater inputs and biological perturbations (see Friis et al., 2003). Empirical model developments that make use of in situ measurement databases will likely continue as the basis for any spaceborne  $T_{\text{alk}}$  algorithms.

## SATELLITE APPROACHES FOR ESTIMATING $p\text{CO}_2$ AND AIR-SEA $\text{CO}_2$ FLUX

The most widely measured upper-ocean carbonate parameter relevant to monitoring carbonate system variability is the  $p\text{CO}_2$  in seawater. This effort began decades ago and has been applied to produce global maps of surface ocean  $p\text{CO}_2$  (e.g., Takahashi et al., 2014). As explained above, when combined with a second ocean  $\text{CO}_2$  system parameter ( $T_{\text{alk}}$ ,  $T_{\text{CO}_2}$ , or pH), knowledge of  $p\text{CO}_2$  allows estimation of calcite and aragonite saturation states, and extensive data sets have been extrapolated to produce global  $\Omega$  maps (Takahashi et al., 2014).

The combination of remote sensing and traditional methods has led to powerful new satellite-based predictive approaches for estimating  $p\text{CO}_2$ . Development and validation of these satellite-based algorithms benefit immensely from in situ surveys and global  $p\text{CO}_2$  monitoring on ships of opportunity and moorings. Comprehensive quality-controlled data repositories such as the Surface Ocean  $\text{CO}_2$  Atlas (SOCAT) and the Lamont-Doherty Earth Observatory (LDEO) databases (Bakker et al., 2014; Takahashi et al., 2014) facilitate access. The satellite products are meant to complement these detailed ground-truth data sets by providing global and regional views (hotspot areas) of the surface ocean with temporal and spatial resolutions far superior to what can be achieved with more traditional methods of collecting data via ship surveys, time-series stations, buoys, and autonomous vehicles.

Moreover, the critically important estimations of air-sea exchange of  $\text{CO}_2$  that constrain global carbon budgets depend on the air-to-sea  $p\text{CO}_2$  disequilibrium. Air-sea flux estimates can be created by combining  $p\text{CO}_2$  disequilibrium with satellite sea state data (often based on wind speed) to estimate  $\text{CO}_2$  gas-exchange coefficients (Wanninkhof, 2014, and preceding studies discussed therein). The combination of remote sensing and traditional methods has led to powerful new

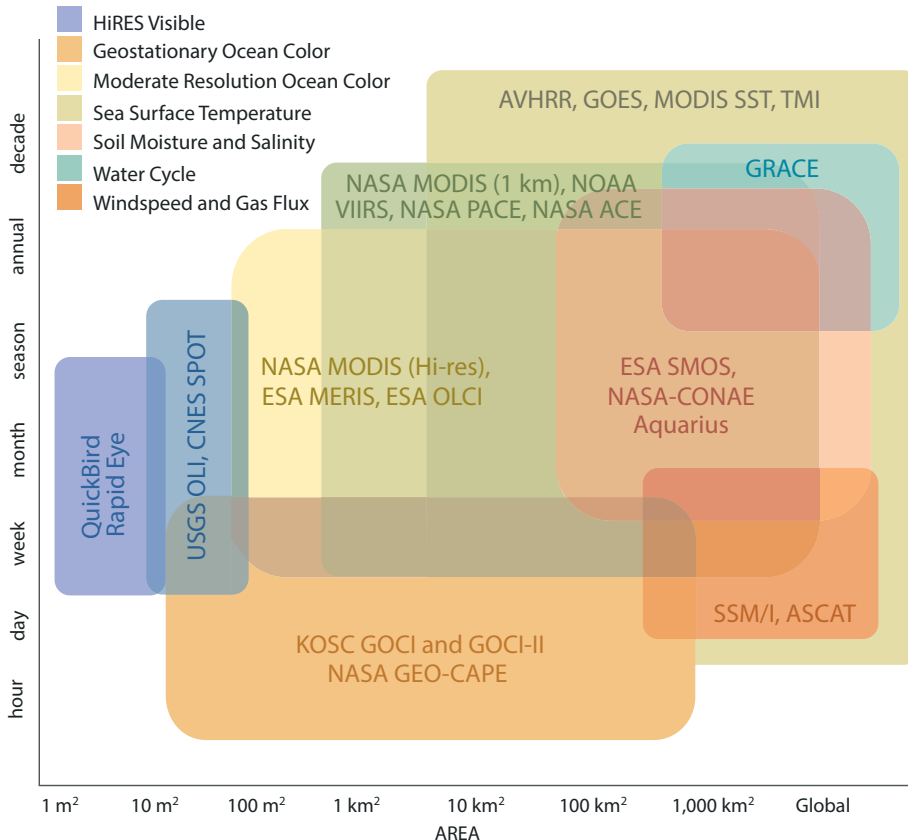


**FIGURE 4.** Coverage by some relevant satellite sensors. Boxes are colored by the variables measured.



satellite-based predictive approaches for estimating  $p\text{CO}_2$  and the air-sea mass flux. At this stage, these approaches rely on SST, ocean color, wind, wave, roughness, and circulation data from the satellites.

Satellite measurements applicable to  $p\text{CO}_2$  algorithm development and validation include SST from the Moderate-resolution Imaging Spectroradiometer (MODIS), Advanced Very High Resolution Radiometer (AVHRR), and other sensors; ocean color products including Chl, primary production, particulate organic and inorganic carbon, dissolved organic carbon derived from the Sea-Viewing Wide Field-of-View Sensor (SeaWiFS), MODIS, MEdium Resolution Imaging Spectrometer (MERIS), and Visible Infrared Imaging Radiometer Suite (VIIRS); and, more recently, salinity from SMOS and Aquarius (see Table 1). These data products provide proxies for physical and biological processes affecting inorganic carbon variability in the ocean, and they have been used to develop

and apply algorithms of  $p\text{CO}_2$  for continental shelves and the deep ocean. These algorithms use a variety of methodologies ranging from multivariate (e.g., Lohrenz and Cai, 2006; Signorini et al., 2013) to statistical methods such as neural networks and self-organizing mapping techniques (Telszewski et al., 2009; Hales et al., 2012) and quasi-mechanistic reconstructions of the underlying  $T_{\text{CO}_2}$  and  $T_{\text{alk}}$  (Hales et al., 2012) that determine  $p\text{CO}_2$ . However, the diversity and complexity of ocean biogeochemical provinces, as well as the steadily increasing surface water  $\text{CO}_2$  levels, suggest that, at this point in time, no single  $p\text{CO}_2$  algorithm will be applicable at the global scale.

The state of the art for these satellite-based algorithms has now reached a stage where they are capable of providing  $\pm 15$  ppmv accuracy in regional  $p\text{CO}_2$  (see studies above). However, in complex coastal regions with large magnitude variation, the accuracy will likely be lower (see Hales et al., 2012).

## REMOTE SENSING OF CALCITE MINERAL SATURATION INDICES, DIC, AND pH

Because net dilution and biological processes affect  $\Omega$ ,  $T_{\text{CO}_2}$ , and pH, we can assume that satellite data analyses will enable reasonable progress toward estimation of such variables. This is the case with  $\Omega$ , where Gledhill et al. (2009) successfully used modeled salinity and remotely sensed SST and wind data to estimate the variability of  $\Omega$  within the greater Caribbean region. We anticipate global  $\Omega$  maps that will utilize satellite-based  $p\text{CO}_2$ , SST, and  $T_{\text{alk}}$  products.

While there are several instances of correlations between remotely observable parameters (Chl, SST, SSS) with  $T_{\text{CO}_2}$  or pH, there is sparse literature on the use of satellite data for  $T_{\text{CO}_2}$  and pH retrievals. This is likely attributable to a weaker covariance with salinity (than  $T_{\text{alk}}$ ) and the fact that visible and thermal data are not robustly correlated with pH or  $T_{\text{CO}_2}$  over larger spatial scales. Nevertheless, regional examples of such correlations are found in the Arctic study of Arrigo et al. (2010), who observed  $T_{\text{CO}_2}$  to be closely related to SST, SSS, and Chl, and Loukos et al. (2000), who estimated  $T_{\text{CO}_2}$  as a function of SST and SSS in the equatorial Pacific. Likewise, Nakano and Watanabe (2005) found a good relationship between pH, SST, and Chl in the North Pacific. Empirical research continues relating commonly observed oceanographic variables, many of which are amenable to remote sensing, to all carbonate system variables (Juranek et al., 2011; Alin et al., 2012).

## REMOTE SENSING OF BIOLOGICAL PROCESSES RELEVANT TO OA

Elevated  $\text{CO}_2$  and reduced pH-related changes in oceanic chemistry can result in changes in primary productivity and food web structure and function (Blackford, 2010; Doney et al., 2012). Satellite-retrievable variables, including SST, photosynthetically available radiation (PAR), Chl, POC, PIC, and

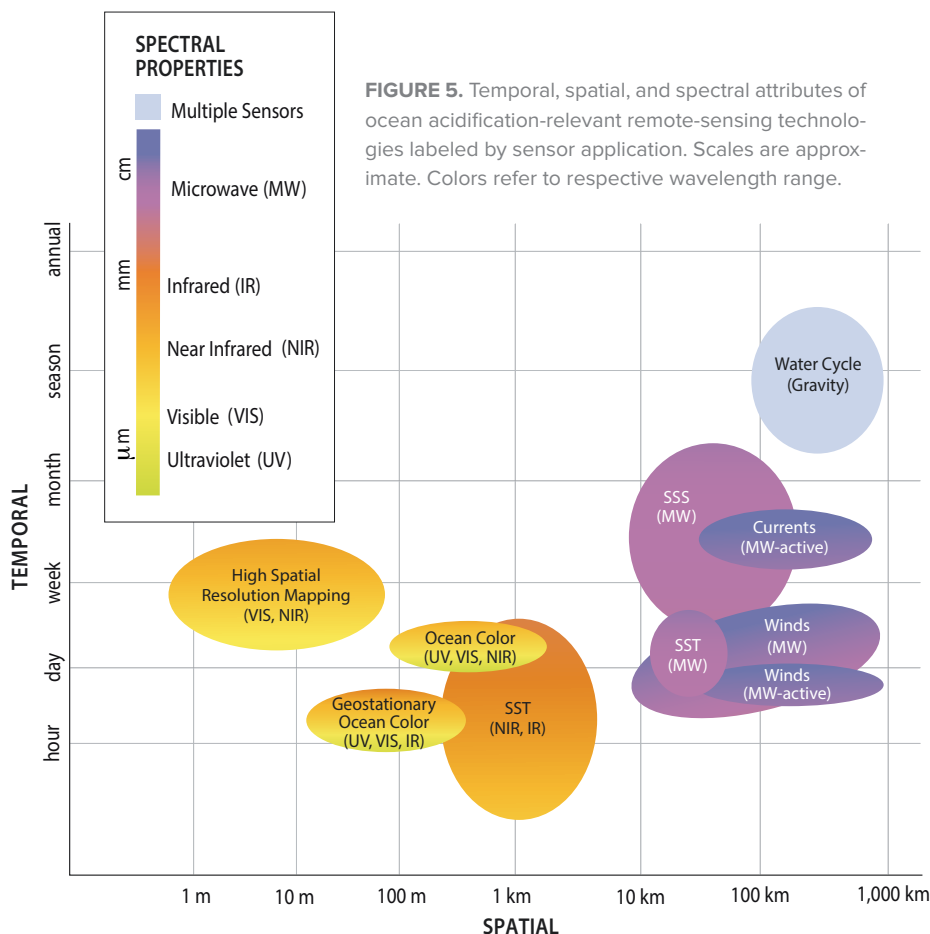


**FIGURE 5.** Temporal, spatial, and spectral attributes of ocean acidification-relevant remote-sensing technologies labeled by sensor application. Scales are approximate. Colors refer to respective wavelength range.

phytoplankton light absorption, are routinely used in algorithms to estimate net primary productivity (NPP) and calcification (Behrenfeld and Falkowski, 1997; Balch et al., 2007). Net community production (NCP; autotrophic fixation of CO<sub>2</sub> minus community respiration), perhaps more relevant to carbon system variability, can also be estimated from satellite observations (Jönsson et al., 2011; Westberry et al., 2012). However, discerning long-term changes in NPP and NCP attributable to carbonate system variability (and vice versa) will be challenging, particularly given the intermingling effects of climate and other sources of variability (e.g., Gattuso and Hansson, 2011).

Changes in pH and seawater carbonate chemistry have been associated with altered rates of growth, photosynthesis, calcification, and N<sub>2</sub> fixation as well as altered bioavailability of nutrients and trace minerals and stoichiometry of biogeochemical processes (Riebesell and Tortell, 2011). It is difficult to generalize how such changes would impact phytoplankton functional types (PFTs; Riebesell and Tortell, 2011).

Satellite observations can be used to infer changes in the functional types that include calcifiers (coccolithophores), silicifiers (diatoms), and nitrogen fixers (cyanobacteria) (IOCCG, 2014). Potential changes or shifts in PFTs may subsequently impact higher trophic levels and the associated cycling of carbon and other elements (Riebesell and Tortell, 2011; Bednaršek et al., 2014). Such satellite data will be useful for refinement and validation of ecosystem model simulations of climate and ocean acidification-related changes in phytoplankton community structure and their impacts on biogeochemical and trophodynamic processes (Dutkiewicz et al., 2013).

Effects on calcification rates have also varied among calcifying plankton, with generally decreasing rates for foraminifera and pteropods in response to elevated CO<sub>2</sub> and reduced pH, but varying responses for coccolithophores (Riebesell and Tortell, 2011). Algorithms

developed for detection of coccolithophores (e.g., Balch et al., 2005) provide a basis for detection and quantification of coccolithophore PIC from satellite observations. Such observations, in turn, are invaluable to carbonate system research in that they provide spatio-temporal information about the conversion of T<sub>CO<sub>2</sub></sub> to PIC (Balch and Utgoff, 2009; Shutler et al., 2013).

Changes in seawater carbon chemistry may also have varying effects on diatoms, as found in both short- and long-term studies (e.g., Tatters et al., 2013; Xu et al., 2014). These silicifiers (diatoms) form large blooms, account for a major fraction of primary production (Rost et al., 2003), and are of particular interest because they strongly influence the vertical flux of particulate material (Buesseler, 1998). Satellite algorithms have been developed that discriminate diatoms from non-diatoms on the basis of differences in spectral properties of these groups (e.g., Sathyendranath et al., 2004).

Recent studies show large variability in CO<sub>2</sub> sensitivity in marine diazotrophs (Hutchins et al., 2013; Eichner et al., 2014). Extensive blooms formed by *Trichodesmium* sp., a diazotrophic (i.e., N<sub>2</sub> fixing) phytoplankton, exhibit various features detectable by satellite (Nair et al., 2008). Satellite estimates of *Trichodesmium* have been used to model regional and global estimates of N<sub>2</sub> fixation (e.g., Westberry et al., 2005). However, these satellite estimates of marine N<sub>2</sub> fixation do not include contributions from some unicellular diazotrophs that also contribute significantly to total nitrogen fixation in some regions (Moisander et al., 2010).

## MIXING PROCESSES

Surface fluxes, surface currents, upwelling, meso- and submesoscale eddies and filaments, internal waves, and transient wind events all impact the transport of water masses and mix their attendant carbonate constituents. Thanks to both high-resolution numerical simulations and satellite observations, a new vision

of upper-ocean dynamics and a deeper understanding of these complex interactions have emerged. Several event-scale processes affecting the vertical transport of carbonate constituents are also amenable to remote sensing.

Based on the small-scale variability in SST and ocean color (e.g., Bennanouz et al., 2014) and/or more accurate surface winds, satellite observations provide new insights about upper-ocean dynamics to reveal vigorous physical and biological processes. Associated vertical fluxes can draw nutrient-rich cold water from the deeper layers into the sunlit (euphotic) zone, where it elicits the rapid growth of phytoplankton, effectively lowering pCO<sub>2</sub> (Hales et al., 2006) and increasing pH during the phytoplankton growth phase.

## Mapping and Change Detection of OA-Sensitive Ecosystems

In addition to aiding understanding of carbonate system variability and its relationship to OA, satellite data are a resource for mapping and change detection of ecosystems sensitive to OA. Remote sensing utilizing radiance from the visible to the near-infrared spectrum has wide applications in mapping changes in extent and condition of shallow-water ecosystems sensitive to OA, such as coral reefs, algae, and macrophyte beds (Andréfouët et al., 2005; Vahtmäe et al., 2006; Brito et al., 2013). Although many of these mapping techniques are limited to quantifying outcomes after bleaching events, the use of thermal imaging satellites provides an early warning system for identifying locations where coral bleaching is likely to occur (Liu et al., 2006).

Early signs of OA impacts on coral reefs may manifest as changes in coral reef processes such as ecosystem productivity and calcification (Kleypas and Yates, 2009). Over time, changes in the rates of these processes can lead to ecosystem transitions characterized by declines in calcifying species such as corals and increases in noncalcifying species such as seagrasses and algae. These ecosystem shifts can lead to loss of topographic complexity

and elevation in reef systems (Kleypas and Yates, 2009) that could be detectable through use of the same satellite and sensor technology used for detecting change due to coral bleaching. However, detecting early signs of OA such as changes in process rates and fine-scale changes in community structure requires significant advancements in the use of multispectral and hyperspectral sensors at submeter spatial resolution.

High-resolution, satellite-based multispectral sensors (e.g., QuickBird-2) and airborne hyperspectral sensors (e.g., Compact Airborne Spectrographic Imager) have been used to successfully map seagrass biodiversity at the individual patch level in shallow coastal waters (Phinn et al., 2008). However, multispectral instruments cannot yet differentiate many reef classes, and most studies of coral reefs using hyperspectral data suitable for characterizing differences among reef components have been limited to in-water data (Andréfouët et al., 2005; Kobryn et al., 2013). Continued improvements in spatial and spectral resolution of hyperspectral sensors are needed for feasible use of satellite platforms for detailed coral reef mapping that could detect impacts of OA on species diversity and ecosystem function.

An early warning system for OA requires the ability to monitor changes in coastal ocean chemistry. Experimental OA satellite products are available for the Caribbean from NOAA's Coral Reef Watch (<http://coralreefwatch.noaa.gov/satellite/oa>; Gledhill et al., 2009; Eakin et al., 2010). These products include  $\Omega$ ,  $p\text{CO}_2$ , total alkalinity, and other carbonate system parameters at 50 km spatial resolution, and are appropriate for open ocean observations. Higher resolution is needed to apply these products to coastal oceans. Efforts are underway to increase spatial resolution and develop algorithms for use in coastal waters.

Recent advances in the development of autonomous in-water sensors for high temporal resolution measurements of carbon system parameters in coastal waters

(Martz et al., 2015, in this issue) present the opportunity to integrate networks of in-water and satellite sensors to link ecosystem processes with satellite-based change detection in reefs. Such integrated sensor networks may be a more feasible interim approach for monitoring coastal carbonate system variability until more cost-effective, satellite-based sensor technology becomes available.

### SENSOR SYNERGY

There are several untapped avenues where satellite data from multiple sensors and platforms may serve to improve our understanding of ocean carbonate system dynamics and acidification. For example, the recently launched NASA Orbiting Carbon Observatory-2 is now retrieving atmospheric  $\text{CO}_2$ , thus providing a new data set for investigations of air-to-sea  $p\text{CO}_2$  disequilibrium. New sensors will also help solve the particular problems and take advantage of opportunities presented in ocean basins that receive large freshwater runoff, largely due to spatial and temporal heterogeneity in carbonate constituent concentrations. Examples include ecosystems contained within the northwestern tropical South Atlantic and the Caribbean with Amazon and Orinoco River discharges, the Bay of Bengal, the Gulf of Mexico, and the Arctic. In all cases, understanding of plume extent and timing, depth of the mixed layer and its wind-impacted advection, and biochemical influx and transformations can all benefit from the spatio-temporal view of salinity, ocean color, wind, and ocean circulation dynamics that can be drawn from the present satellite complement.

Gravity sensor missions such as GRACE allow mapping of continental water budgets, enabling or validating estimates of gross freshwater flux to the coast. Discharge estimates can be constrained using data from soil moisture missions such as SMOS, Soil Moisture Active Passive (SMAP), and Advanced Microwave Scanning Radiometer-EOS (AMSR-E) (Hirpa et al., 2014). Furthermore, salinity missions such as SMOS

and Aquarius presently allow mapping of this discharge into the coastal ocean and beyond (e.g., Gierach et al., 2013; Le Vine et al., 2014), albeit at scales of  $\sim 100$  km. Close to the coast where pixel size limitations hamper salinity sensor capabilities, it is possible to retrieve salinity at higher resolution from established regional relationships between salinity and ocean color variables (Mollerli et al., 2010; Salisbury et al., 2011; Reul et al., 2013). Using surface current data generated with satellite altimeters and wind products derived from scatterometers, it is also possible to remotely track the evolution of surface water masses to further understand the sources and fates of carbonate constituents.

Within the context of a moving water mass, bio-optical approaches may be employed to estimate biological perturbations to carbonate parameters along the flow path, including those that are not conservative with salinity. Examples include using NPP or NCP products to estimate net  $T_{\text{CO}_2}$  uptake and calcification products (e.g., Balch et al., 2011) that estimate net total alkalinity removal and  $T_{\text{CO}_2}$  production by PIC-producing phytoplankton. Newer hyperspectral data will have increased potential to evaluate PFT distributions, and thus could provide information on the potential for nitrogen fixation via cyanobacteria or effects of OA on various phytoplankton groups. Geostationary platforms such as the Geostationary Ocean Color Imager (GOCI) allow important insights into diurnal variability of NPP and mixing of coastal water masses (Lee et al., 2012; Lee et al., 2013).

Such synergy opens the possibility for vastly improved  $T_{\text{alk}}$ ,  $\Omega$ , and  $p\text{CO}_2$  algorithms that, when cast globally, are likely to perform poorly due to a differing covariance between inputs. Regional approaches can be envisioned whereby terms related to spatio-temporal variability of processes affecting  $\text{CO}_2$  and calcite solubility, mixing, and biological rates can be estimated using various satellite data streams. Finally, we note

opportunities to capitalize on the spatial and temporal attributes of satellite data streams for filling gaps in time and space. One such approach described by Velo et al. (2013) and used to interpolate the GLObal Ocean Data Analysis Project (GLODAP) and the CARbon dioxide IN the Atlantic Ocean (CARINA)  $T_{alk}$  data could reasonably be modified to incorporate satellite temperature fields.

## FUTURE DIRECTIONS

Satellite missions recently launched or those that are in advanced planning stages will undoubtedly further our understanding of OA. Using only ocean color sensors as an example, Table 2 highlights several satellite missions that will be realized in the coming decade. Many other sensors relevant to OA studies (but not shown)

are in the planning stages and will provide better spatial, temporal, or spectral resolution that will continue present climate data records or initiate new types of OA-relevant data streams. For example, the US National Research Council recommends several future mission concepts relevant to study of the carbonate system (NRC, 2007), and the European Union has recently begun the 6 billion euro Copernicus Programme, designed to provide long-term monitoring of the environment with its fleet of Sentinel satellites. These missions will enable new investigations of atmospheric  $CO_2$ , will provide improved  $CO_2$  and calcite mineral solubility estimates, and will improve our knowledge of freshwater cycling, its spatio-temporal evolution, and its impacts on, and interactions with, coastal acidification.

Future missions are poised to fill important gaps in our understanding of the biological impacts on acidification, including resolution of diurnal processes and identification of phytoplankton functional groups that have differential effects on surface carbonate chemistry. They promise to advance our understanding of the role of high discharge and upwelling-influenced regions that will certainly require more complex algorithms using multiple satellite data streams.

Resolving dynamic coastal processes affecting carbonate parameters at regional and basin scales will require high frequency (hourly to bihourly) ocean color and SST satellite observations that can only be provided by geostationary sensors. Coastal ocean color observations from a geostationary orbit will

**TABLE 2.** Planned satellite missions relevant to carbonate system variability and OA, using ocean color missions as an example. The planned ocean color missions highlight the advances in spatial, spectral, and temporal resolution that can be used to understand various interactions of biology and OA. Missions dedicated to complementary geophysical measurements such as sea surface temperature, wave height, sea state, and visible mapping are also planned.

SENSOR	AGENCY	SATELLITE	SCHEDULED LAUNCH	SPATIAL RESOLUTION (m)	# OF BANDS	ORBIT	SPECTRAL COVERAGE (nm)
OLCI	ESA/ EUMETSAT	Sentinel 3A	2015	300/1,200	21	Polar	400–1,020
COCTS CZI	CNSA (China)	HY-1C/D (China)	2015	1,100 250	10 10	Polar	402–12,500 433–885
SGLI	JAXA (Japan)	GCOM-C	2016	250/1,000	19	Polar	375–12,500
COCTS CZI	CNSA (China)	HY-1E/F (China)	2017	1,100 250	10 4	Polar	402–12,500 433–885
HSI	DLR (Germany)	EnMAP	2017	30	242	Polar	420–2,450
OCM-3	ISRO (India)	OCEANSAT-3	2017	360/1	13	Polar	400–1,010
OLCI	ESA/ EUMETSAT	Sentinel-3B	2017	260	21	Polar	390–1,040
VIIRS	NOAA/NASA (USA)	JPSS-1	2017	370/740	22	Polar	402–11,800
Multi-Spectral Optical Camera	INPE/CONAE	SABIA-MAR	2018	200/1,100	16	Polar	380–11,800
GOCI-II	KARI/KIOST (South Korea)	GeoKompsat 2B	2018	250/1,000	13	Geo	412–1,240 TBD
OCI	NASA	PACE	2018	TBD	TBD	Polar	TBD
Coastal Ocean Color Imaging Spec (Name TBD)	NASA	GEO-CAPE	>2022	250–375	155 TBD	Geo	340–2,160

OLCI = Ocean and Land Colour Instrument  
 COCTS CZI = Chinese Ocean Color and Temperature Scanner (COCTS)  
 and Coastal Zone Imager (CZI)  
 SGLI = Second-Generation Global Imager  
 HIS = Hyperspectral Imager

OCM-3 = Ocean Colour Monitor  
 VIIRS = Visible Infrared Imaging Radiometer Suite  
 GOCI-II = Geostationary Ocean Color Imager  
 OCI = Ocean-Color Imager




be critical for observing ecosystem processes that have life cycles on time scales ranging from minutes to hours to a few days. Geostationary orbit (~36,000 km altitude) offers unprecedented and virtually continuous temporal coverage (e.g., the Geostationary Operational Environmental Satellite [GOES] Imager collects images every 30 minutes). This capability is necessary for studying large bays and coastal oceans where physical, biological, and chemical processes react on short time scales. Enhanced frequency in coverage will yield an unparalleled number of clear-sky retrievals of ocean color compared to the one to three images per week (at best) for most sites from low Earth orbiting (LEO) sensors such as the MODIS and VIIRS sensors, or the planned Pre-Aerosol Cloud and ocean Ecology (PACE) mission.

While increasing analyses of satellite data will aid in our understanding of carbonate system variability and acidification processes, many challenges remain. It is important to reiterate that, presently, information gained from satellite data is generally limited to the surface or mixed layer. As such, our community will still need to continue data collection efforts aimed at understanding subsurface processes as well as the biogeochemical connectivity between the mixed layer and deeper waters. Increased spectral, spatial, and temporal resolution will require new retrieval algorithms, atmospheric corrections, data handling, and geo-location techniques. Many satellite data streams are currently subject to considerable error (e.g.,  $\pm 0.3^\circ\text{C}$  for SST [Corlett et al., 2014] and  $\pm \sim 30\%$  for Chl [Gregg and Casey, 2004]). Thus, future validation data efforts will require simultaneous carbonate system parameters and the geophysical variables that are measured remotely. Examples include moored time series, autonomous platforms, and more traditional cruises that offer the opportunity for higher data quality control. Finally, we recommend that the community move quickly toward the development of robust, inexpensive carbonate system,

biological, bio-optical, and geophysical sensors that can be deployed throughout the world ocean. These technologies would help constrain the  $\text{CO}_2$  system parameters in both time and space, contributing significantly to needed satellite calibration and validation efforts.

## SUMMARY

A constellation of satellites designed to retrieve various data streams related to ocean physics, biology, and chemistry presently provides insights into OA and carbonate system variability. These data are useful for understanding various processes, including  $\text{CO}_2$  and calcite mineral saturation states, rates of biological  $\text{T}_{\text{CO}_2}$  uptake, spatio-temporal distributions of surface alkalinity, and processes related to horizontal and vertical mixing of carbonate parameters. A fuller understanding of OA variability will be realized as present data streams are synthesized and as satellite data are validated using in situ observations from moored and mobile platforms. Satellite missions scheduled to be launched or those that are in mature planning phases will provide new data streams, including atmospheric  $\text{CO}_2$  and hydrologic variability, and will also provide improvements to current data streams by virtue of better spatial, temporal, or spectral resolution. 

**ACKNOWLEDGMENTS.** We gratefully acknowledge our sponsors whose grants made this collaboration possible. The NASA Ocean Biology & Biogeochemistry program (particularly NNX14AL84G), the NOAA Ocean Acidification Program and Integrated Ocean Observing System programs, including Northeastern Regional Association of Coastal Ocean Observing Systems (NERACOOS) grants A002004 and USM-GR05194-001, Pathfinder ESA-STSE Ocean Acidification, and the National Science Foundation. Background and satellite images in Figure 1 are courtesy of NASA, except the GOCI satellite image, which is courtesy of the Korea Ocean Satellite Research Center and the SMOS satellite image, which is courtesy of the European Space Agency. Aquarius is a joint mission shared by NASA and CONAE. We appreciate the insightful critiques of Frank Muller-Karger, Nick Hardman-Mountford, and one anonymous reviewer, and thank Amy Ehntholt and Kristy Donahue for valuable help. References to non-USGS products and services are provided for information only and do not constitute endorsement or warranty, expressed or implied, by the US Government, as to their suitability, content, usefulness, functioning, completeness, or accuracy. We acknowledge funding support from the National Oceanic and Atmospheric Administration (NOAA)'s Ocean Acidification Program and NOAA's Pacific Marine Environmental Laboratory (PMEL contribution number 4303).

## REFERENCES

- Alin, S.R., R.A. Feely, A.G. Dickson, J.M. Hernández-Ayón, L.W. Juranek, M.D. Ohman, and R. Goericke. 2012. Robust empirical relationships for estimating the carbonate system in the southern California Current System and application to CalCOFI hydrographic cruise data (2005–2011). *Journal of Geophysical Research* 117(C5), <http://dx.doi.org/10.1029/2011JC007511>.
- Andréfouët, S., E.J. Hochberg, C. Cheillon, F.E. Muller-Karger, J.C. Brock, and C. Hu. 2005. Multi-scale remote sensing of coral reefs. Pp. 297–315 in *Remote Sensing of Coastal Aquatic Environments: Technologies, Techniques, and Applications*, vol. 7. R.L. Miller, C.E. Del Castillo, and B.A. McKee, eds, Springer, [http://dx.doi.org/10.1007/978-1-4020-3100-7\\_13](http://dx.doi.org/10.1007/978-1-4020-3100-7_13).
- Arrigo, K.R., S. Pabi, G.L. van Dijken, and W. Maslowski. 2010. Air-sea flux of  $\text{CO}_2$  in the Arctic Ocean, 1998–2003. *Journal of Geophysical Research* 115, G04024, <http://dx.doi.org/10.1029/2009JG001224>.
- Bakker, D.C.E., B. Pfeil, K. Smith, S. Hankin, A. Olsen, S.R. Alin, C. Cosca, S. Harasawa, A. Kozyr, Y. Nojiri, and others. 2014. An update to the Surface Ocean  $\text{CO}_2$  Atlas (SOCAT version 2). *Earth System Science Data* 6:69–90, <http://dx.doi.org/10.5194/essd-6-69-2014>.
- Balch, W.M., D. Drapeau, B. Bowler, and E. Booth. 2007. Prediction of pelagic calcification rates using satellite measurements. *Deep Sea Research* 54:478–495, <http://dx.doi.org/10.1016/j.dsr2.2006.12.006>.
- Balch, W.M., D.T. Drapeau, B.C. Bowler, E. Lyczkowski, E.S. Booth, and D. Alley. 2011. The contribution of coccolithophores to the optical and inorganic carbon budgets during the Southern Ocean Gas Exchange Experiment: New evidence in support of the “Great Calcite Belt” hypothesis. *Journal of Geophysical Research* 116, C00F06, <http://dx.doi.org/10.1029/2011JC006941>.
- Balch, W.M., H.R. Gordon, B.C. Bowler, D.T. Drapeau, and E.S. Booth. 2005. Calcium carbonate measurements in the surface global ocean based on Moderate-Resolution Imaging Spectroradiometer data. *Journal of Geophysical Research* 110, C07001, <http://dx.doi.org/10.1029/2004JC002560>.
- Balch, W.M., and P.E. Utgoff. 2009. Potential interactions among ocean acidification, coccolithophores, and the optical properties of seawater. *Oceanography* 22(4):146–159, <http://dx.doi.org/10.5670/oceanog.2009.104>.
- Bednaršek, N., R.A. Feely, J.C.P. Reum, B. Peterson, J. Menkel, S.R. Alin, and B. Hales. 2014. *Limacina helicina* shell dissolution as an indicator of declining habitat suitability owing to ocean acidification in the California Current Ecosystem. *Proceedings of the Royal Society B* 281(1785), <http://dx.doi.org/10.1098/rspb.2014.0123>.
- Behrenfeld, M.J., and P.G. Falkowski. 1997. A consumer's guide to phytoplankton primary productivity models. *Limnology and Oceanography* 42:1479–1491, <http://dx.doi.org/10.4319/lo.1997.42.7.1479>.
- Benazzouz, A., S. Mordane, A. Orbi, M. Chagdali, K. Hilmi, A. Atillah, J.L. Pelegri, and D. Hervé. 2014. An improved coastal upwelling index from sea surface temperature using satellite-based approach: The case of the Canary Current upwelling system. *Continental Shelf Research* 81:38–54, <http://dx.doi.org/10.1016/j.csr.2014.03.012>.
- Blackford, J.C. 2010. Predicting the impacts of ocean acidification: Challenges from an ecosystem perspective. *Journal of Marine Systems* 81:12–18, <http://dx.doi.org/10.1016/j.jmarsys.2009.12.016>.
- Breitburg, D.L., J. Salisbury, J.M. Bernhard, W.-J. Cai, S. Dupont, S.C. Doney, K.J. Kroeker, L.A. Levin, W.C. Long, L.M. Milke, and others. 2015. And on top of all that... Coping with ocean acidification in the midst of many stressors. *Oceanography* 28(2):48–61, <http://dx.doi.org/10.5670/oceanog.2015.31>.
- Brito, A.C., I. Benyoucef, B. Jesus, V. Brotas, P. Gemez, C.R. Mendes, P. Launeau, M.P. Dias, and L. Barillé. 2013. Seasonality of microphytobenthos revealed by remote-sensing in a South European estuary. *Continental Shelf Research* 66:83–91, <http://dx.doi.org/10.1016/j.csr.2013.07.004>.

- Buesseler, K.O. 1998. The decoupling of production and particulate export in the surface ocean. *Global Biogeochemical Cycles* 12:297–310, <http://dx.doi.org/10.1029/97GB03366>.
- Cai, W.-J., X. Hu, W.-J. Huang, L.-Q. Jiang, Y. Wang, T.-H. Peng, and X. Zhang. 2010. Alkalinity distribution in the western North Atlantic Ocean margins. *Journal of Geophysical Research* 115, C08014, <http://dx.doi.org/10.1029/2009JC005482>.
- Cooley, S.R., H.L. Kite-Powell, and S.C. Doney. 2009. Ocean acidification's potential to alter global marine ecosystem services. *Oceanography* 22(4):172–181, <http://dx.doi.org/10.5670/oceanog.2009.106>.
- Corlett, G.K., C.J. Merchant, P.J. Minnett, and C.J. Donlon. 2014. Assessment of long-term satellite derived sea surface temperature records. *Experimental Methods in the Physical Sciences* 47:639–677, <http://dx.doi.org/10.1016/B978-0-12-417011-7.00021-0>.
- Cross, J.N., J.T. Mathis, N.R. Bates, and R.H. Byrne. 2013. Conservative and non-conservative variations of total alkalinity on the southeastern Bering Sea shelf. *Marine Chemistry* 154:100–112, <http://dx.doi.org/10.1016/j.marchem.2013.05.012>.
- Del Castillo, C.E., and R.L. Miller. 2008. On the use of ocean color remote sensing to measure the transport of dissolved organic carbon by the Mississippi River Plume. *Remote Sensing of the Environment* 112:836–844, <http://dx.doi.org/10.1016/j.rse.2007.06.015>.
- Doney, S.C., V.J. Fabry, R.A. Feely, and J.A. Kleypas. 2009. Ocean acidification: The other CO<sub>2</sub> problem. *Annual Review of Marine Science* 1:169–192, <http://dx.doi.org/10.1146/annurev.marine.010908.163834>.
- Doney, S.C., M. Ruckelshaus, J.E. Duffy, J.P. Barry, F. Chan, C.A. English, H.M. Galindo, J.M. Grebmeier, A.B. Hollowed, N. Knowlton, and others. 2012. Climate change impacts on marine ecosystems. *Annual Review of Marine Science* 4:11–37, <http://dx.doi.org/10.1146/annurev-marine-041911-111611>.
- Dutkiewicz, S., J.R. Scott, and M.J. Follows. 2013. Winners and losers: Ecological and biogeochemical changes in a warming ocean. *Global Biogeochemical Cycles* 27:463–477, <http://dx.doi.org/10.1002/gbc.20042>.
- Eakin, C.M., J.A. Morgan, S.F. Heron, T.B. Smith, G. Liu, L. Alvarez-Filip, B. Baca, E. Bartels, C. Bastidas, C. Bouchon, and others. 2010. Caribbean corals in crisis: Record thermal stress, bleaching, and mortality in 2005. *PLoS ONE* 5(11), <http://dx.doi.org/10.1371/journal.pone.0013969>.
- Eichner, M., B. Rost, and S.A. Kranz. 2014. Diversity of ocean acidification effects on marine N<sub>2</sub> fixers. *Journal of Experimental Marine Biology and Ecology* 457:199–207, <http://dx.doi.org/10.1016/j.jembe.2014.04.015>.
- Emery, W.J., D.J. Baldwin, P. Schlüssel, and R.W. Reynolds. 2001. Accuracy of in situ sea surface temperatures used to calibrate infrared satellite measurements. *Journal Of Geophysical Research* 106(C2):2,387–2,405, <http://dx.doi.org/10.1029/2000JC000246>.
- Feely, R.A., C.L. Sabine, R.H. Byrne, F.J. Millero, A.G. Dickson, R. Wanninkhof, A. Murata, L.A. Miller, and D. Greeley. 2012. Decadal changes in the aragonite and calcite saturation state of the Pacific Ocean. *Global Biogeochemical Cycles* 26, GB3001, <http://dx.doi.org/10.1029/2011GB004157>.
- Feely, R.A., C.L. Sabine, J.M. Hernandez-Ayon, D. Ianson, and B. Hales. 2008. Evidence for upwelling of corrosive “acidified” water onto the continental shelf. *Science* 320:1,490–1,492, <http://dx.doi.org/10.1126/science.1155676>.
- Friis, K., A. Kortzinger, and D.W.R. Wallace. 2003. The salinity normalization of marine inorganic carbon chemistry data. *Geophysical Research Letters* 30, 1085, <http://dx.doi.org/10.1029/2002GL015898>.
- Gattuso, J.-P., and L. Hansson. 2011. *Ocean Acidification*. Oxford University Press, Oxford and New York, 408 pp.
- Gierach, M.M., J. Vasquez-Cuervo, T. Lee, and V.M. Tsontos. 2013. Aquarius and SMOS detect effects of an extreme Mississippi River flooding event in the Gulf of Mexico. *Geophysical Research Letters* 40:5,188–5,193, <http://dx.doi.org/10.1002/grl.50995>.
- Gledhill, D., R. Wanninkhof, and M. Eakin. 2009. Observing ocean acidification from space. *Oceanography* 22(4):48–59, <http://dx.doi.org/10.5670/oceanog.2009.96>.
- Gregg, W.W., and N.W. Casey. 2004. Global and regional evaluation of the SeaWiFS chlorophyll data set. *Remote Sensing of Environment* 93:463–479, <http://dx.doi.org/10.1016/j.rse.2003.12.012>.
- Hales, B., L. Karp-Boss, A. Perlin, and P.A. Wheeler. 2006. Oxygen production and carbon sequestration in an upwelling coastal margin. *Global Biogeochemical Cycles* GB001, <http://dx.doi.org/10.1029/2005GB002517>.
- Hales, B., P.G. Stratton, M. Saraceno, R. Letelier, T. Takahashi, R. Feely, C. Sabine, and F. Chavez. 2012. Satellite-based prediction of pCO<sub>2</sub> in coastal waters of the eastern North Pacific. *Progress in Oceanography* 103:1–15, <http://dx.doi.org/10.1016/j.pocean.2012.03.001>.
- Hardman-Mountford, N.J., G. Moore, D.C.E. Bakker, A.J. Watson, U. Schuster, R. Barciela, A. Hines, G. Monofioffé, J. Brown, S. Dye, and others. 2008. An operational monitoring system to provide indicators of CO<sub>2</sub>-related variables in the ocean. *ICES Journal of Marine Science* 65:1,498–1,503, <http://dx.doi.org/10.1093/icesjms/fsn110>.
- Hirpa, F.A., M. Gebremichael, T.M. Hopson, R. Wojcik, and H. Lee. 2014. Assimilation of satellite soil moisture retrievals into a hydrologic model for improving river discharge. Pp. 319–329 in *Remote Sensing of the Terrestrial Water Cycle*. V. Lakshmi, D. Alsdorf, M. Anderson, S. Biancamaria, M. Cosh, J. Entin, G. Huffman, W. Kustas, P. van Oevelen, T. Painter, J. Parajka, M. Rodell, and C. Rüdiger, eds, John Wiley & Sons, Inc, Hoboken, NJ.
- Horrazabal, S., G. Shaffer, J. Letelier, and O. Ulloa. 2001. Local and remote forcing of sea surface temperature in the coastal upwelling system off Chile. *Journal of Geophysical Research* 106(C8):16,657–16,671, <http://dx.doi.org/10.1029/2001JC900008>.
- Hutchins, D.A., F.X. Fu, E.A. Webb, N. Walworth, and A. Tagliabue. 2013. Taxon-specific response of marine nitrogen fixers to elevated carbon dioxide concentrations. *Nature Geoscience* 6:790–795, <http://dx.doi.org/10.1038/ngeo1858>.
- IOCCG (International Ocean-Colour Coordinating Group). 2014. *Phytoplankton Functional Types from Space*. S. Sathyendranath, ed., Reports of the International Ocean-Colour Coordinating Group No. 15, IOCCG, Dartmouth, Canada, 163 pp., [http://www.ioccg.org/reports/IOCCG\\_Report\\_15\\_2014.pdf](http://www.ioccg.org/reports/IOCCG_Report_15_2014.pdf).
- IPCC (Intergovernmental Panel on Climate Change). 2013. *Climate Change 2013: The Physical Science Basis. Contribution of Working Group I to the Fifth Assessment Report of the Intergovernmental Panel on Climate Change*. T.F. Stocker, D. Qin, G.-K. Plattner, M. Tignor, S.K. Allen, J. Boschung, A. Nauels, Y. Xia, V. Bex, and P.M. Midgley, eds, Cambridge University Press, Cambridge, United Kingdom and New York, NY, USA, 1,535 pp.
- Jönsson, B.F., J.E. Salisbury, and A. Mahadevan. 2011. Large variability in continental shelf production of phytoplankton carbon revealed by satellite. *Biogeosciences* 8:1,213–1,223, <http://dx.doi.org/10.5194/bg-8-1213-2011>.
- Juranek, L.W., R.A. Feely, D. Gilbert, H. Freeland, and L.A. Miller. 2011. Real-time estimation of pH and aragonite saturation state from Argo profiling floats: Prospects for an autonomous carbon observing strategy. *Geophysical Research Letters* 38(17), <http://dx.doi.org/10.1029/2011GL048580>.
- Key, R.M., A. Kozyr, C. Sabine, K. Lee, R. Wanninkhof, J.L. Bullister, R.A. Feely, F. Millero, C. Mordy, and T. Peng. 2004. A global ocean carbon climatology: Results from Global Data Analysis Project (GLDAP). *Global Biogeochemical Cycles* 18, GB4031, <http://dx.doi.org/10.1029/2004GB002247>.
- Kleypas, J.A., and K.K. Yates. 2009. Coral reefs and ocean acidification. *Oceanography* 22(4):108–117, <http://dx.doi.org/10.5670/oceanog.2009.101>.
- Kobryn, H.T., K. Wouters, L.E. Beckley, and T. Heege. 2013. Ningaloo Reef: Shallow marine habitats mapped using a hyperspectral sensor. *PLoS ONE* 8(7), <http://dx.doi.org/10.1371/journal.pone.0070105>.
- Lagerloef, G., S. Yueh, and J. Piepmeiner. 2013. NASA's Aquarius Mission provides new ocean view. *Sea Technology* January 2013, <http://www.sea-technology.com/features/2013/0113/NASA.php>.
- Land, P.E., J.D. Shutler, H.S. Findlay, F. Girard-Arduin, R. Sabia, N. Reul, J.-F. Piolle, B. Chapron, Y. Quifien, J.E. Salisbury, and others. 2015. Salinity from space unlocks satellite-based assessment of ocean acidification. *Environmental Science & Technology* 49:1,987–1,994, <http://dx.doi.org/10.1021/es504849s>.
- Lee, Z., M. Jiang, C. Davis, N. Pahlevan, Y.-H. Ahn, and R. Ma. 2012. Impact of multiple satellite ocean color samplings in a day on assessing phytoplankton dynamics. *Ocean Science Journal* 47:323–329, <http://dx.doi.org/10.1007/s12601-012-0031-5>.
- Lee, H.J., J.Y. Park, S.H. Lee, J.M. Lee, and T.K. Kim. 2013. Suspended sediment transport in a rock-bound, macrotidal estuary: Han Estuary, eastern Yellow Sea. *Journal of Coastal Research* 29:358–371, <http://dx.doi.org/10.2112/JCOASTRES-D-12-00066.1>.
- Lee, K., T. Tong, F.J. Millero, C.L. Sabine, A.G. Dickson, C. Goyet, G.-H. Park, R. Wanninkhof, R.A. Feely, and R.M. Key. 2006. Global relationships of total alkalinity with salinity and temperature in surface waters of the world's oceans. *Geophysical Research Letters* 33, L19605, <http://dx.doi.org/10.1029/2006GL027207>.
- Lefèvre, N., J. Aiken, J. Rutllant, G. Daneri, S. Lavender, and T. Smyth. 2002. Observations of pCO<sub>2</sub> in the coastal upwelling off Chile: Spatial and temporal extrapolation using satellite data. *Journal of Geophysical Research* 107(C6), <http://dx.doi.org/10.1029/2000JC000395>.
- Lefèvre, N., A.J. Watson, and A.R. Watson. 2005. A comparison of multiple regression and neural network techniques for mapping in situ pCO<sub>2</sub> data. *Tellus Series B* 57:375–384, <http://dx.doi.org/10.1111/j.1600-0889.2005.00164.x>.
- Le Quéré, C., R. Moriarty, R.M. Andrew, G.P. Peters, P. Ciais, P. Friedlingstein, S.D. Jones, S. Sitch, P. Tans, A. Arnett, and others. 2014. Global carbon budget 2014. *Earth System Science Data Discussions* 7:521–610, <http://dx.doi.org/10.5194/essdd-7-521-2014>.
- Le Vine, D.M., E.P. Dinnat, G.S.E. Lagerloef, P. de Matthes, S. Abraham, C. Utku, and H. Kao. 2014. Aquarius: Status and recent results. *Radio Science* 49:709–720, <http://dx.doi.org/10.1002/2014RS005505>.
- Liu, C., R. Miller, K.L. Carder, Z.P. Lee, E. D'Sa, and J. Ivey. 2006. Estimating the underwater light field from remote sensing of ocean color. *Journal of Oceanography* 62:235–248, <http://dx.doi.org/10.1007/s10872-006-0048-4>.
- Lohrenz, S.E., and W.-J. Cai. 2006. Satellite ocean color assessment of air-sea fluxes of CO<sub>2</sub> in a river-dominated coastal margin. *Geophysical Research Letters* 33, L01601, <http://dx.doi.org/10.1029/2005GL023942>.
- Loukos, H., F. Vivier, P.P. Murphy, D.E. Harrison, and C. Le Quéré. 2000. Interannual variability of equatorial Pacific CO<sub>2</sub> fluxes estimated from temperature and salinity data. *Geophysical Research Letters* 27:1,735–1,738, <http://dx.doi.org/10.1029/1999GL011013>.
- Martz, T.R., K.L. Daly, R.H. Byrne, J.H. Stillman, and D. Turk. 2015. Technology for ocean acidification research: Needs and availability. *Oceanography* 28(2):40–47, <http://dx.doi.org/10.5670/oceanog.2015.30>.
- Mathis, J.T., J.N. Cross, N. Monacci, R.A. Feely, and P. Staben. 2014. Evidence of prolonged aragonite undersaturations in the bottom waters of the southern Bering Sea shelf from autonomous sensors. *Deep Sea Research Part II* 109:125–133, <http://dx.doi.org/10.1016/j.dsr2.2013.07.019>.
- Moisander, P.H., R.A. Beinart, I. Hewson, A.E. White, K.S. Johnson, C.A. Carlson, J.P. Montoya, and J.P. Zehr. 2010. Unicellular cyanobacterial

- distributions broaden the oceanic N<sub>2</sub> fixation domain. *Science* 327:1,512–1,514, <http://dx.doi.org/10.1126/science.1185468>.
- Moller, G.S.F., E.M.L. de M. Novo, and M. Kampel. 2010. Space-time variability of the Amazon River plume based on satellite ocean color. *Continental Shelf Research* 30:342–352, <http://dx.doi.org/10.1016/j.csr.2009.11.015>.
- Mumby, P.J., J. Chisholm, A.J. Edwards, C.D. Clark, E.B. Roark, S. Andréfouët, and J. Jaubert. 2001. Unprecedented bleaching-induced mortality in *Porites* spp. at Rangiroa Atoll, French Polynesia. *Marine Biology* 139:183–189, <http://dx.doi.org/10.1007/s002270100575>.
- Nair, A., S. Sathyendranath, T. Platt, J. Morales, V. Stuart, M.-H. Forget, E. Devred, and H. Bouman. 2008. Remote sensing of phytoplankton functional types. *Remote Sensing of the Environment* 112:3,366–3,375, <http://dx.doi.org/10.1016/j.rse.2008.01.021>.
- Nakano, Y., and Y.W. Watanabe. 2005. Reconstruction of pH in the surface seawater over the North Pacific basin for all seasons using temperature and chlorophyll-*a*. *Journal of Oceanography* 61:673–680, <http://dx.doi.org/10.1007/s10872-005-0075-6>.
- NRC (National Research Council). 2007. *Earth Science and Applications from Space: National Imperatives for the Next Decade and Beyond*. Committee on Earth Science and Applications from Space: A Community Assessment and Strategy for the Future. National Academies Press, Washington, DC, 456 pp.
- Phinn, S., C. Roelfsema, A. Dekker, V. Brando, and J. Anstee. 2008. Mapping seagrass species, cover and biomass in shallow waters: An assessment of satellite multi-spectral and airborne hyper-spectral imaging systems in Moreton Bay (Australia). *Remote Sensing of the Environment* 112:3,413–3,425, <http://dx.doi.org/10.1016/j.rse.2007.09.017>.
- Reul, N., S. Fournier, J. Boutin, O. Hernandez, C. Maes, B. Chapron, G. Alory, Y. Quilfen, J. Tenerelli, and S. Morisset. 2013. Sea surface salinity observations from space with the SMOS satellite: A new means to monitor the marine branch of the water cycle. *Surveys in Geophysics* 35:681–722, <http://dx.doi.org/10.1007/s10712-013-9244-0>.
- Reynolds, R.W., C.L. Gentemann, and G.K. Corlett. 2010. Evaluation of AATSR and TMI Satellite SST Data. *Journal of Climate* 23:152–165, <http://dx.doi.org/10.1175/2009JCLI3252.1>.
- Riebesell, U., and P.D. Tortell. 2011. Effects of ocean acidification on pelagic organisms and ecosystems. Pp. 99–121 in *Ocean Acidification*. J.-P. Gattuso and L. Hansson, eds. Oxford University Press, Oxford.
- Rödenbeck, C., R.F. Keeling, D.C.E. Bakker, N. Metz, A. Olsen, C. Sabine, and M. Heimann. 2013. Global surface-ocean pCO<sub>2</sub> and sea-air CO<sub>2</sub> flux variability from an observation-driven ocean mixed-layer scheme. *Ocean Science* 9:193–216, <http://dx.doi.org/10.5194/os-9-193-2013>.
- Rost, B., U. Riebesell, A. Burkhardt, and D. Sultemeyer. 2003. Carbon acquisition of bloom-forming marine phytoplankton. *Limnology and Oceanography* 48:55–67, <http://dx.doi.org/10.4319/lo.2003.48.1.0055>.
- Sabine, C.L., and T. Tanhua. 2010. Estimation of anthropogenic CO<sub>2</sub> inventories in the ocean. *Annual Review of Marine Science* 2:175–198, <http://dx.doi.org/10.1146/annurev-marine-120308-080947>.
- Salisbury, J.E., M. Green, C. Hunt, and J.W. Campbell. 2008. Coastal acidification by rivers: A threat to shellfish? *Eos, Transactions American Geophysical Union* 89:513, <http://dx.doi.org/10.1029/2008EO50001>.
- Salisbury, J.E., D. Vandemark, J. Campbell, C. Hunt, D. Wisser, N. Reul, and B. Chapron. 2011. Spatial and temporal coherence between Amazon River discharge, salinity, and light absorption by colored organic carbon in western tropical Atlantic surface waters. *Journal of Geophysical Research* 116, C00H02, <http://dx.doi.org/10.1029/2011JC006989>.
- Sarmiento, J.L., and N. Gruber. 2006. *Ocean Biogeochemical Dynamics*. Princeton University Press, Princeton, NJ, 528 pp.
- Sathyendranath, S., L. Watts, E. Devred, T. Platt, C. Caverhill, and H. Maass. 2004. Discrimination of diatoms from other phytoplankton using ocean-colour data. *Marine Ecology Progress Series* 272:59–68, <http://dx.doi.org/10.3354/meps272059>.
- Signorini, S., R.A. Mannino, R.G. Najjar, M.A.M. Friedrichs, W.-J. Cai, J. Salisbury, Z.A. Wang, H. Thomas, and E. Shadwick. 2013. Surface ocean pCO<sub>2</sub> seasonality and sea-air CO<sub>2</sub> flux estimates for the North American east coast. *Journal of Geophysical Research* 118:5,439–5,460, <http://dx.doi.org/10.1002/jgrc.20369>.
- Shutler, J.D., P.E. Land, C.W. Brown, H.S. Findlay, C.J. Donlon, M. Medland, R. Snooke, and J.C. Blackford. 2013. Coccolithophore surface distributions in the North Atlantic and their modulation of the air-sea flux of CO<sub>2</sub> from 10 years of satellite Earth observation data. *Biogeosciences* 10:2,699–2,709, <http://dx.doi.org/10.5194/bg-10-2699-2013>.
- Takahashi, T., S.C. Sutherland, D.W. Chipman, J.G. Goddard, C. Ho, T. Newberger, C. Sweeney, and D.R. Munro. 2014. Climatological distributions of pH, pCO<sub>2</sub>, total CO<sub>2</sub>, alkalinity, and CaCO<sub>3</sub> saturation in the global surface ocean, and temporal changes at selected locations. *Marine Chemistry* 164:95–125, <http://dx.doi.org/10.1016/j.marchem.2014.06.004>.
- Tatters, A.O., M.Y. Røleda, A. Schnetzer, F. Fu, C.L. Hurd, P.W. Boyd, D.A. Caron, A.A.Y. Lie, L.J. Hoffmann, and D.A. Hutchins. 2013. Short- and long-term conditioning of a temperate marine diatom community to acidification and warming. *Philosophical Transactions of the Royal Society B*, <http://dx.doi.org/10.1098/rstb.2012.0437>.
- Telszewski, M., A. Chazottes, U. Schuster, A.J. Watson, C. Moulin, D.C.E. Bakker, M. González-Dávila, T. Johannessen, A. Körtzinger, H. Lüger, and others. 2009. Estimating the monthly pCO<sub>2</sub> distribution in the North Atlantic using a self-organizing neural network. *Biogeosciences* 6:1,405–1,421, <http://dx.doi.org/10.5194/bg-6-1405-2009>.
- Vahtmäe, E., T. Kutser, G. Martin, and J. Kotta. 2006. Feasibility of hyperspectral remote sensing for mapping benthic macroalgal cover in turbid coastal waters: A Baltic Sea case study. *Remote Sensing of Environment* 101:342–351, <http://dx.doi.org/10.1016/j.rse.2006.01.009>.
- Velo, A., F.F. Pérez, T. Tanhua, M. Gilcoto, A.F. Rios, and R.M. Key. 2013. Total alkalinity estimation using MLR and neural network techniques. *Journal of Marine Systems* 111–122:11–18, <http://dx.doi.org/10.1016/j.jmarsys.2012.09.002>.
- Waldbusser, G.G., and J.E. Salisbury. 2014. Ocean acidification in the coastal zone from an organism's perspective: Multiple system parameters, frequency domains, and habitats. *Annual Review of Marine Science* 6:221–247, <http://dx.doi.org/10.1146/annurev-marine-121211-172238>.
- Wanninkhof, R. 2014. Relationship between wind speed and gas exchange over the ocean revisited. *Limnology and Oceanography: Methods* 12(6):351–362, <http://dx.doi.org/10.4319/lom.2014.12.351>.
- Westberry, T.K., D.A. Siegel, and A. Subramaniam. 2005. An improved bio-optical model for the remote sensing of *Trichodesmium* spp. blooms. *Journal of Geophysical Research* 110, C06012, <http://dx.doi.org/10.1029/2004JC002517>.
- Westberry, T.K., P.J.L.B. Williams, and M.J. Behrenfeld. 2012. Global net community production and the putative net heterotrophy of the oligotrophic oceans. *Global Biogeochemical Cycles* 26, GB4019, <http://dx.doi.org/10.1029/2011GB004094>.
- Xu, D., Y. Wang, X. Fan, D. Wang, N. Ye, X. Zhang, S. Mou, Z. Guan, and Z. Zhuang. 2014. Long-term experiment on physiological responses to synergetic effects of ocean acidification and photoperiod in the Antarctic sea ice algae *Chlamydomonas* sp. ICE-L. *Environmental Science & Technology* 48:7738–7746, <http://dx.doi.org/10.1021/es404866z>.
- Zeebe, R.E., and D. Wolf-Gladrow. 2001. *CO<sub>2</sub> in Seawater: Equilibrium, Kinetics, 1996*. Elsevier Oceanography Series, 65, 360 pp.

## APPENDIX

This appendix contains rough estimates of the time it would take to track sensible changes in pCO<sub>2</sub> and Ω using present satellite data and algorithms.

Given the assumptions:

- Satellite pCO<sub>2</sub> algorithm error = ±15 μatm (typical open ocean, from Lefèvre et al., 2005; Telszewski et al., 2009; Hales et al., 2012; and others)
- Satellite salinity error = ±0.2; (Reul et al., 2013, for SMOS)
- Satellite SST error = ±0.3°C (typical, from Emery et al., 2001; Reynolds et al., 2010)
- T<sub>alk</sub> algorithm error, using in situ SST and SSS = ±8.1 μmol kg<sup>-1</sup> (Lee et al., 2006)

**pCO<sub>2</sub>:** The current rate of pCO<sub>2</sub> change over the globe is ~2–2.5 ppm per year. Given the overall ±15 μatm error in estimating pCO<sub>2</sub> using remote sensing methods, it will take six to eight years of constant change in pCO<sub>2</sub> to detect a significant change in pCO<sub>2</sub>.

**Ω:** To examine the time needed to track a change in Ω, we performed a Monte Carlo analysis assuming random distributions of the errors. Note that the SST and salinity impart error to both the solubility and the total alkalinity algorithms. The result of 1,000 Monte Carlo trials yields a Ω error of 0.11 using the assumptions above. Thus, in order to track the annual change in Ω of 0.01–0.016 units (depending on the rate of CO<sub>2</sub> increase [2–2.5 ppm]), we need about a decade, perhaps less, to discern a change.

**AUTHORS.** Joseph Salisbury (joe.salisbury@unh.edu) is Research Assistant Professor, Ocean Processes Analysis Laboratory, University of New Hampshire, Durham, NH, USA. Douglas Vandemark is Research Professor, Ocean Processes Analysis Laboratory, University of New Hampshire, Durham, NH, USA. Bror Jönsson is Associate Research Scholar, Geosciences, Princeton University, Princeton, NJ, USA. William Balch is Senior Research Scientist, Bigelow Laboratory for Ocean Sciences, East Boothbay, ME, USA. Sumit Chakraborty is Postdoctoral Researcher, School for Marine Science and Technology, University of Massachusetts Dartmouth, New Bedford, MA, USA. Steven Lohrenz is Dean, School for Marine Science and Technology, University of Massachusetts Dartmouth, New Bedford, MA, USA. Bertrand Chapron is a researcher at the Laboratoire d’Océanographie Spatiale IFREMER, Plouzané, France. Burke Hales is Professor, College of Earth, Ocean, and Atmospheric Sciences, Oregon State University, Corvallis, OR, USA. Antonio Mannino is Oceanographer, Ocean Ecology Division, NASA Goddard Space Flight Center, Greenbelt, MD, USA. Jeremy T. Mathis is Supervisory Oceanographer, National Oceanic and Atmospheric Administration (NOAA), Pacific Marine Environmental Laboratory, Seattle, WA, USA. Nicolas Reul is a researcher at the Laboratoire d’Océanographie Spatiale IFREMER, La Seyne-sur-Mer Cedex, France. Sergio R. Signorini was Senior Scientist/Analyst, Science Applications International Corporation, McLean, VA, USA, and is Senior Scientist, Goddard Space Flight Center, National Aeronautics and Space Administration, Greenbelt, MD, USA. Rik Wanninkhof is Oceanographer, NOAA Atlantic Oceanographic and Meteorological Laboratory, Miami, FL, USA. Kimberly K. Yates is Research Oceanographer, US Geological Survey, St. Petersburg, FL, USA.

## ARTICLE CITATION

Salisbury, J., D. Vandemark, B. Jönsson, W. Balch, S. Chakraborty, S. Lohrenz, B. Chapron, B. Hales, A. Mannino, J.T. Mathis, N. Reul, S.R. Signorini, R. Wanninkhof, and K.K. Yates. 2015. How can present and future satellite missions support scientific studies that address ocean acidification? *Oceanography* 28(2):108–121, <http://dx.doi.org/10.5670/oceanog.2015.35>.